VERSITA

Arch. Min. Sci., Vol. 57 (2012), No 3, p. 547–577

Electronic version (in color) of this paper is available: http://mining.archives.pl

DOI 10.2478/v10267-012-0036-z

ILIE ONICA*, DACIAN MARIAN*

GROUND SURFACE SUBSIDENCE AS EFFECT OF UNDERGROUND MINING OF THE THICK COAL SEAMS IN THE JIU VALLEY BASIN

OSIADANIE GRUNTÓW WSKUTEK WYBIERANIA POKŁADÓW O DUŻEJ MIĄŻSZOŚCI W KOPALNIACH ZAGŁĘBIA W DOLINIE JIU

In the case of the thick and gentle coal seam no. 3 of the Jiu Valley Coal Basin (Romania), the mining methods are by use of the longwall mining technologies with roof control by caving or top coal caving. In this paper, it is presented the analysis of the complex deformations of the ground surface, over time, as a consequence of the coal mining in certain mining fields of the basin. Also, it is analysed the ground surface subsidence phenomenon using the CESAR-LCPC finite element code. The modelling is made in the elasticity and the elasto-plasticity behaviour hypothesis. Also, the time dependent analysis of the ground surface deformation was achieved with the aid of an especial profile function. The obtained results are compared with the in situ measurements data basis.

Keywords: subsidence, displacement, profile function, finite element method, elasticity, elasto-plasticity

W przypadku delikatnego pokładu węgla nr 3, o dużej miąższości, eksploatowanego w Zagłębiu Węglowym Jiu w Rumunii, wydobycie prowadzi się metodą ścianową z prowadzeniem stropu na zawał. W pracy tej przedstawiono analizę złożonych odkształceń powierzchni gruntu w funkcji czasu, spowodowanej podziemnych eksploatacją kolejnych pól węglowych. Przebadano także zjawisko osiadania terenu przy użyciu metody elementów skończonych z wykorzystaniem kodu CESAR-LCPC. Modelowanie przeprowadzono przy przyjętej hipotezie zachowania sprężystego i sprężysto-plastycznego gruntu. Przeprowadzono także analizę zmiennych w czasie odkształceń terenu w oparciu o wyprowadzone funkcje profilu osiadania. Otrzymane rezultaty porównano z wynikami pomiarów dokonanych *in situ*.

Słowa kluczowe: osiadanie, przemieszczenie, funkcja profilu osiadania, metoda elementów skończonych, sprężystość, zachowanie sprężysto –plastyczne

* UNIVERSITY OF PETROŞANI, UNIVERSITY STREET, NO. 20, ROMANIA

The Petroşani Hard Coal Basin of Romania contains a balance reserve of about one billion tonnes of coal. The intensive coal mining of this deposit began after the Second World War, reaching after 1980 over 9-10 millions tonnes of coal per year. Due to Romanian industry reorganisation, after the year 1990, in conformity with the new demands of the market economy, the coal production of this basin was reduced to about 3.5 million tonnes per year. From the beginning this coal deposit was split into 16 mining fields, from which following several successive reorganisation and closing stages, only 7 mining fields are left in activity. In this coal basin the most economical importance have the coal seam no. 3 (48%) and coal seam no. 5 (12%). As the deposit genesis is sedimentary, the most frequent rocks in the basin are: limestones, marls, argillaceous or marly sandstones, conglomerates, etc.- rocks of relatively low stability. In these conditions has arisen the necessity of revaluation of the impact produced by the underground mining on the ground surface; to determine the development of the subsidence phenomenon in view to elaborate some of the prevention methodologies and the design of the safety pillars for some objectives situated on the surface and underground. Therefore, besides starting the new subsidence and displacement measurements, in the first stage, we proceeded to analyse the old measurements achieved at the Hard Coal Company level, along the time, in different mining fields. Having in view the great diversity of the geo-mining conditions of the mined zones (thick coal seams with gentle and great dip, situated at the variable depths), the most significant cases were taken in study. After the analysis of these measurements, it was elaborated a special time dependent profile function for the conditions of gentle and medium dip seams, as Uricani mine, and generalized for the great dip mines, as Vulcan, Lonea, Petrila, Dâlja mines, with a very good precision of the results. Also, for all these mines, was modified the profile function elaborated by Peng and Chen (Peng & Chen, 1981) for Northern Appalachian Coalfield, taking into account the time factor. The numerical modelling of the subsidence phenomenon, for the conditions of the thick coal seams with gentle and medium dip (for example, the Livezeni and Uricani mines cases) was achieved with the aid of CESAR-LCPC finite element code. The calculus in 2D was made in the plain strain hypothesis, in elasticity and elasto-plasticity, for the Mohr-Coulomb without hardening rock mass behaviour; in both behaviour hypothesis, the results are close. Because of the very important sizes of the models, the 3D modelling calculus was achieved only in the elasticity behaviour hypothesis. In the Livezeni mine case was analysed the effect superposition of three adjacent mining panels on the ground surface stability; and for the case of the Uricani mine, only the effect of a single panel. For both cases, was modelled the dynamic development of the subsidence basin as panel mining extension in view to establish the subsidence stage, respectively subcritical, critical and supracritical subsidence.

1. Generalities

The Petroşani Hard Coal Basin, under the management of the Hard Coal Company of Petroşani, contains the most important hard coal deposit of Romania, with a balance reserve of about one billion tonnes of coal. This coal deposit was known and mined since the year 1788, as far back as the Austro-Hungarian Empire (Almăşan, 1984). But, the intensive coal mining of this deposit began at the same time with Romania's industrialisation, after the Second World War, reaching after 1980 over 9-10 millions tonnes of coal per year (Almăşan, 1984; Petrescu, 1987).

Due to Romanian industry reorganisation, after the year 1990, in conformity with the new demands of the market economy, the coal production of this basin was reduced to about 3.5 million tonnes per year.

From the beginning this coal deposit was split into 16 mining fields, from which following several successive reorganisation and closing stages, only 7 mining fields are left in activity.

The complicated deposit tectonics determines the delimitation in geological blocks of reduced extent (most of them varying between 200 and 300 m) and an equally technical difficulty in mining. Moreover, there occurs a methane gas emission (of over 10 to 15 methane m^3/coal tonne) and there is a marked tendency of coal self-ignition (Almăşan, 1984; Petrescu, 1987).

In this coal basin, through the geological research works, there was identified a number of 18 coal seams, of which the most economical importance having the coal seam no. 3 (48%) and coal seam no. 5 (12%). The sedimentary rocks complex, in which these coal seams are present, consists in rocks deposits which belong to Superior Cretaceous, Neocene and the Quaternary (Petrescu, 1987).

As the deposit genesis is sedimentary, the most frequent rocks in the basin are: limestones, marls, argillaceous or marly sandstones, conglomerates, etc., their strength ranging between 15-16 MPa up 50-60 MPa, sometimes even more. Mainly, they are rocks of relatively low stability (Onica & Cozma, 2008).

The main factors that contribute at the definition of the stress and strain state surrounding the excavations generated by the coal seams mining with the roof rocks caving, in the Jiu Valley coal basin, are the following: the excavation sizes, the seam dip, the coal and surrounding geo-mechanics characteristics, the mining depth, the face supports characteristics, the face advancement speed, the distance from the adjacent panels, the distance from nearby coal seams, etc (Oncioiu & Onica, 1999; Onica & Cozma, 2008).

The average values of the main mechanical and elastic characteristics of the rocks used in the ground surface deformation analysis, in the Livezeni Mine conditions, are shown in the Table 1 (Hirean, 1981; Todorescu, 1984).

TABLE 1

The average values of the geo-mechanical characteristics of the roof and floor rocks of the coal seam no. 3 (Hirean, 1981; Todorescu, 1984)

Rock characteristic	**UM**	**Rock**		**Coal seam no. 3**
		roof	**floor**	
Apparent specific weight, γ_a	kN/m^3	26.63	27.01	14.5
Young modulus of elasticity, E	kN/m^2	5 035 000	5 268 000	1 035 000
Poisson ratio, ν	–	0,19	0,20	0,13
Compressive strength, σ_c	kN/m^2	43 500	46 000	12 500
Tensile strength, σ_t	kN/m^2	4 600	4 950	1 000
Cohesion, C	kN/m^2	6 130	6 630	1 300
Internal friction angle, φ	^{o}	55	56	50

As a result of the measurement analysis made on the ground surface under the underground mining influence, so as to find the optimum design parameters of the main safety pillars, the limit angles of subsidence have been set for the different coal mining fields of the Jiu Valley Coal Basin. Thus, the values of the limit angles of influence (β, γ and δ) – measured from the horizontal

line, depending on the mining depth H (m), in conformity with the instructions elaborated by the ICPMC Petroşani are expressed by the following relations (Ortelecan, 1997):

$$\beta = 0.0309 \cdot H + 56.8\,; \quad \gamma = 0.0261 \cdot H + 56.133\,; \quad \delta = 0.146 \cdot H + 51.867$$

Also, in the same conditions, the average failure angles, recommended by ICPMC are the following:

$$\beta_{failure} = 45 \div 55^\circ\,; \quad \gamma_{failure} = 55 \div 60^\circ\,; \quad \delta_{failure} = 75^\circ$$

The subject of this study consists in the underground mining influence analysis on the ground surface of the coal seam no. 3 in the case Uricani, Vulcan, Lonea, Petrila and Dâlja mines, by using a newly developed profile function. Also, at the Livezeni and Uricani mines we have made a numerical modelling of the subsidence phenomenon using the CESAR-LCPC finite element software.

2. Ground surface deformation as effect of longwall mining of the coal seam no. 3 of the Livezeni Mine

The subject of this study consists in the underground mining influence analysis on the ground surface of three adjacent mining panels (panel (3-4), panel 5 and panel 6), situated on the coal seam no. 3, block VI A, Livezeni Mine. Coal seam no. 3, for these panels, was mined in inclined slices (about 2.5 m thickness) with the longwall mining system, complexly- mechanized (powered support SMA-P2H, shearer 2K52-MY and armoured conveyer TR-7) and roof control by caving (Covaci, 1983). The underground excavations sizes results from the coal mining corresponding of these panels are presented into Table 2.

TABLE 2

The average sizes of the mining panel of the coal seam no. 3, block VI A, Livezeni Mine

Panel	Slices number	Total thickness of mined seam (m)	Longwall face length (m)	Panel extent (m)
Panel (3-4)	4	10	119	346
Panel 5	5	12.5	87	440
Panel 6	1	2.5	137	362

2.1. Ground surface deformation monitoring

Now, the monitoring of the ground surface deformation parameters under the underground mining influence at the Livezeni Mine is made using a monitoring (surveying) station that consists in 50 benchmarks. The benchmarks' emplacement is along the access road toward the Parâng Mountains tourist area (Ortelecan & Pop, 2005). The topographical measurements were made every three months, beginning with the year 2001. This monitoring station provides data concerning the ground subsidence area affected by the mining of the coal seam no. 3, block IV A, panel (3-4), 5 and 6. Taking into account the values of the measured parameters, with the aid of the known calculus relations, there were determined the main parameters of the subsidence basin, namely: subsidence or vertical displacement, horizontal displacement, horizontal strain and the slope (Onica, 2001b; Onica et al., 2006).

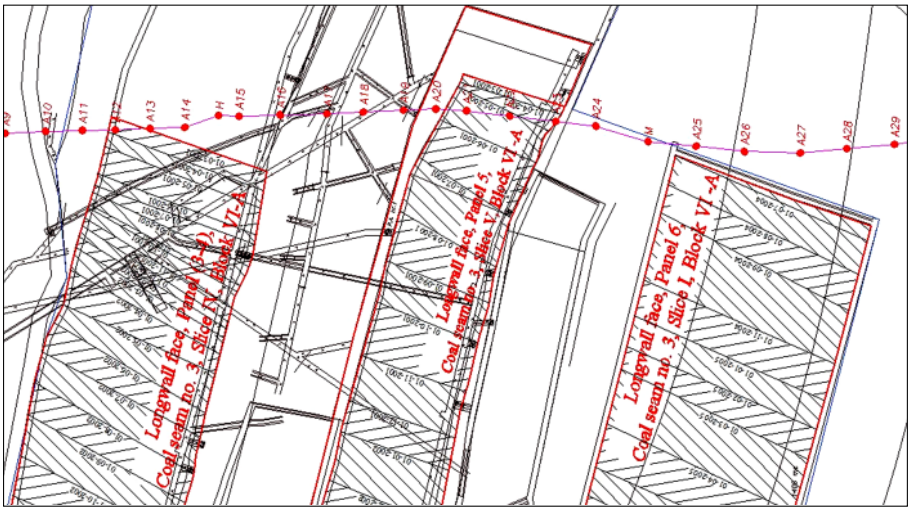

Fig. 1. Monitoring station of ground displacement and deformation of Livezeni Mine

The subsidence basin from the Figure 2 is a composed basin, resulted from the superposition influence of the three panels. This subsidence basin has an irregular shape due the fact that the three individual basin are intersected, and also because the monitoring station is situated toward the mining boundaries of the panels (Fig. 1), area where the transversal deviations are maximum.

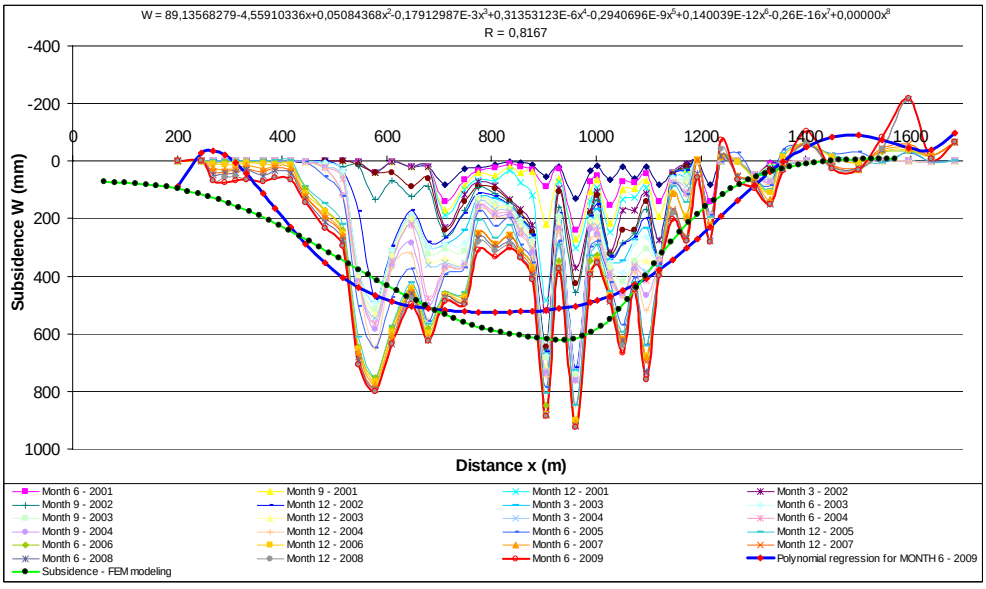

Fig. 2. Subsidence profiles at the Livezeni Mine

In this case, the accuracy of the values that characterise the obtained subsidence basin is lower because the fact that, it is not only the result of the ground subsidence but also the result of the displacement of it, and the deviations were corrected in conformity with a methodology. Even if the transversal deviations that act on this subsidence profile are approximately equal in all the points situated inside the goaf, the difference level between every point benchmark at the base measurement and the their level at the final measurement is not the same, because the ground surface elevation mark is different .

Analysing the in situ measurements situation, we can conclude that, taking into account the ground surface subsidence and displacements there are some cases of the correction determination of the measured values. These adjustments of the measured values are necessary only in the case when the horizontal displacement and (or) the transversal deviation are significant and when the ground surface is inclined.

In the case of this monitoring (surveying) station, the maximum measured subsidence is of $W_{max} = 924$ mm and the horizontal displacement ranges between the value of $U = +3712$ mm and $U = -3625$ mm. The average of maximum subsidence is $W_{max} = 524$ mm (the reference value in the case of numerical modelling).

2.2. Numerical modelling of the subsidence phenomenon

2.2.1. 2D finite element modelling of the subsidence phenomenon

2.2.1.1. Model description

To build the 2D finite element calculus models the CESAR-LCPC finite element code was used. The CESAR software, development of which began in 1981, is the successor of the ROSA-LIE system developed by the Central Laboratory of Bridges and Roads of Paris, between 1963 and 1983. CESAR is a computational general code, based on the finite element method, addressed to the following areas: structures; soils and rocks mechanics; thermo-mechanics; hydrogeology. The CESAR-LCPC code, version 4, which involves the Cleo2D and Cleo3D processors, completed with the C0 option (linear and non-linear static mechanics & diffusion) was used in this work, to perform the following models.

To determine the displacement and the ground surface deformation in the case of Livezeni Mine, where the ground is affected by the three panels, there were made two different models, in the plane strain hypothesis, namely: 1) the model "with mining voids" resulted as a consequence of underground coal mining; 2) the model "with caved zones" (on a height equal to eight times the mined height), due the roof rocks caving in the goaf (Fig. 3).

The calculus for these two models was performed in two hypotheses: a) in the elastic behaviour of the rock massive and b) in the Mohr-Coulomb elasto-plastic without hardening behaviour.

In view of finding the influence degree of every panel on the entire subsidence basin, generated by mining all of these three panels, maintaining the geo-mechanical conditions constant, there were made certain models where the coal seam mining was simulated with every independent panel.

In all of the modelling cases, both rocks and coal seam no. 3 were supposed to be continuous, homogenous and isotropic and the geo-mechanical characteristics taken into the calculus having the average values (Tab. 1).

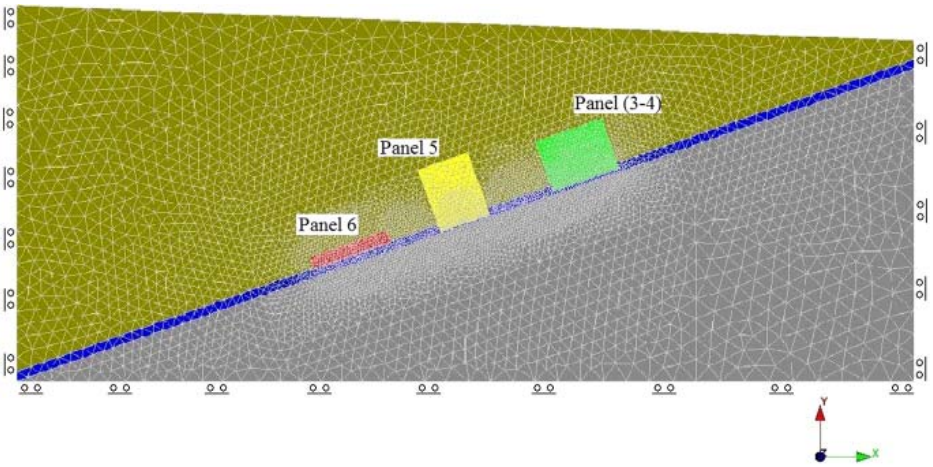

Fig. 3. Finite element model "with caved zones"

The natural state of stresses was estimated being geostatic, characterized by the vertical stress $\sigma_v = \gamma \cdot H$ and horizontal stress $\sigma_h = \frac{\nu}{1-\nu} \cdot \sigma_v$ (because of the lack of the real values in situ measured).

To fit on the models in function of the measured values of the maximum vertical displacements and to correct the rocks and coal characteristics in laboratory obtained (Tab. 1) toward the in situ values, the calculus of the models was made successively using the values reduced by 0%, 30%, 50% and 70% (respectively multiplied with a reducing coefficient K = 1; 0,7; 0,5; 0,3 – structural weakness coefficient). Because the numerical models were significantly sensitive only to the modulus of elasticity variation, only the reduction of this parameter was taken into analysis.

2.2.1.2. Modelling achievement

2D modelling achievement, in the plane strain hypothesis, for every previous defined model the following steps were necessary: a) establishment of boundaries, interest zones and meshing of the model; b) determination of zones (regions) and computational hypothesis and the geomechanical characteristics input; c) boundaries conditions establishment; d) initial conditions and loading conditions establishment; e) achievement of calculus and stoking of results (Onica, 2001a).

For a better precision of the calculus, the models were performed with sizes X = 1500 m and Y = 690 m. Also, the sizes of the interest zone around underground excavations were established so as to involve the model surface where the stress and strain variation is maximum. Model meshing, respectively of every region, was made by triangle finite elements with quadratic interpolation. Respectively, the model meshing was performed with a total number of nodes of 23 448 and surface elements of 11 661.

In order to make a qualitative description of the models, there were taken into consideration 3 regions with various geo-mechanical characteristics, in the case of the models "with mining voids", respectively 4 regions in the case of the models "with caved zones", adequate at the roof and floor rocks, coal seam and the caved rocks of the goaf.

The rocks characteristics, considered to be homogenous and isotropic, are presented in Table 1, and taken in the calculus in the elastic behaviour hypothesis, respectively elasto- plastically without hardening behaviour Mohr-Coulomb hypothesis, were reduced successively, taking into account the structural weakness coefficient.

The caved rocks of the goaf was considered being a very compressible elastic body, characterized by the elasticity modulus of 5 000 kN/m^2, Poisson ratio of 0.4 and specific density of 1800 kg/m^3.

The superior side of the model is considered free and the lateral sides, blocked (for the inferior side the vertical displacements $v = 0$ and the horizontals $u \neq 0$ and for the lateral sides $v \neq 0$ and $u = 0$).

Initial loading conditions of the model were considered as geostatic $[\sigma_o]$, corresponding to an average mining depth of $H = 337$ m, namely: the vertical geostatic stresses

$$\sigma_{oy} = \rho_s \cdot g \cdot H = 87818 \text{ kN/m}^2 = 87.8 \text{ MPa}$$

and the horizontal geostatic stresses

$$\sigma_{ox} = \frac{\nu}{1-\nu} \cdot \sigma_{oy} = k_o \cdot \sigma_{oy} = 21076 \text{ kN/m}^2 = 21.076 \text{ MPa (where: } k_o = \frac{\nu}{1-\nu} = 0.24).$$

The induced stress by the excavation presence was $[\sigma_e]$, respectively the stresses variation represented by the horizontal stress $\sigma_{ex} = -21.076$ MPa and the vertical stress $\sigma_{ey} = -87.8$ MPa. Thus, the loading of the model was performed in the total stresses: $[\sigma_T] = [\sigma_o] - [\sigma_e]$ (Onica, 2001a).

The calculus was made taking 60 iterations per increment and a tolerance of 1% of the results, using for the resolution the initial stress method with non-linear behaviour of geo-mechanical problem.

The calculus results were stocked in the graphical form on the model surface (isovalue, vector and tensor representation) and in the predefined sections following the ground surface. The results obtained are corresponding to the subsidence W (mm) and horizontal displacement U (mm).

2.2.1.3. Analysis of the numerical modelling results

Analyzing the obtained results from the numerical modelling it is observed that the surface basin has a simple shape, different by report to the real basin, because of their emplacement toward the goaf boundaries. In contrary, in the case of FEM modelling, the profile is situated in the middle part of the subsidence basin.

The maximum subsidence and displacements values obtained from the numerical modelling, in elasticity and elasto- plasticity, previous presented, are shown in table 3.

From the previous table it could be observed that, there are very small differences between the models computed in elasticity and the same ones in elasto-plasticity behaviour (the rocks having behaviour to the limits between these). The results more appropriate to the in situ measurement are for the "caved zones" models, in elasto-plasticity behaviour, for a structural weakness coefficient of $K = 0.5$.

In the Figure 4 are represented the subsidence basins obtained for the models "with caved zones", in elasto-plasticity (for $K = 0.5$), as result of three panels mining, as well as the subsidence basin generated by the every singular panel and various combinations between them, and the horizontal displacements curves are shown in Figure 5.

TABLE 3

Maximum subsidence and displacements obtained from the numerical modelling for individual mining panel and for grouped mining panels

ELASTICITY – Models "with mining voids"												
Coef.	**Panel 6**			**Panel 5**			**Panel (3-4)**			**Panel (3-4) + 5 + 6**		
	W	***U***		***W***	***U***		***W***	***U***		***W***	***U***	
	Max.	**Max.**	**Min.**	**Max.**	**Max.**	**Min.**	**Max.**	**Max.**	**Min.**	**Max.**	**Max.**	**Min.**
	mm	**mm**	**mm**	**mm**	**mm**	**mm**	**mm**	**mm**	**mm**	**mm**	**mm**	**mm**
$K = 1$	–155	46	–46	–66	24	–19	–74	28	–19	–237	78	–71
$K = 0,7$	–221	65	–66	–95	34	–27	–106	40	–27	–339	111	–101
$K = 0,5$	–310	92	–92	–133	48	–37	–148	55	–37	–474	156	–142
$K = 0,3$	–516	153	–153	–222	80	–62	–247	92	–62	–790	260	–237
ELASTO-PLASTICITY – Models "with mining voids"												
Coef.	**Panel 6**			**Panel 5**			**Panel (3-4)**			**Panel (3-4) + 5 + 6**		
	W	***U***		***W***	***U***		***W***	***U***		***W***	***U***	
	Max.	**Max.**	**Min.**	**Max.**	**Max.**	**Min.**	**Max.**	**Max.**	**Min.**	**Max.**	**Max.**	**Min.**
	mm	**mm**	**mm**	**mm**	**mm**	**mm**	**mm**	**mm**	**mm**	**mm**	**mm**	**mm**
$K = 1$	–158	47	–47	–68	24	–19	–74	28	–19	–241	79	–72
$K = 0,7$	–226	67	–67	–97	35	–27	–107	40	–27	–344	113	–103
$K = 0,5$	–317	94	–94	–135	48	–38	–149	55	–37	–482	158	–144
$K = 0,3$	–528	157	–156	–225	81	–63	–248	92	–62	–803	264	–240
ELASTICITY – Models "with caved zones"												
Coef.	**Panel 6**			**Panel 5**			**Panel (3-4)**			**Panel (3-4) + 5 + 6**		
	W	***U***		***W***	***U***		***W***	***U***		***W***	***U***	
	Max.	**Max.**	**Min.**	**Max.**	**Max.**	**Min.**	**Max.**	**Max.**	**Min.**	**Max.**	**Max.**	**Min.**
	mm	**mm**	**mm**	**mm**	**mm**	**mm**	**mm**	**mm**	**mm**	**mm**	**mm**	**mm**
$K = 1$	–160	47	–49	–104	25	–41	–87	25	–28	–309	68	–121
$K = 0,7$	–229	67	–69	–148	36	–58	–125	36	–40	–442	97	–173
$K = 0,5$	320	93	–97	–208	50	–82	–175	51	–56	–619	136	–242
$K = 0,3$	–534	156	–162	–346	84	–136	–291	84	–94	–1032	226	–404
ELASTO-PLASTICITY – Models "with caved zones"												
Coef.	**Panel 6**			**Panel 5**			**Panel (3-4)**			**Panel (3-4) + 5 + 6**		
	W	***U***		***W***	***U***		***W***	***U***		***W***	***U***	
	Max.	**Max.**	**Min.**	**Max.**	**Max.**	**Min.**	**Max.**	**Max.**	**Min.**	**Max.**	**Max.**	**Min.**
	mm	**mm**	**mm**	**mm**	**mm**	**mm**	**mm**	**mm**	**mm**	**mm**	**mm**	**mm**
$K = 1$	–156	46	–47	–104	25	–41	–87	25	–28	–310	68	–122
$K = 0,7$	–218	64	–65	–148	36	–58	–125	36	–40	–444	98	–174
$K = 0,5$	–312	92	–94	–208	50	–82	–175	51	–56	–621	137	–243
$K = 0,3$	–521	153	–156	–346	84	–136	–291	84	–94	–1035	228	–405

The subsidence basins obtained from the numerical (FEM) modelling on the model "with mining voids" and on the model "with caving zones", for all that three mining panels, in elasticity and elasto-plasticity, for a structural weakness coefficient of $K = 0.5$ are presented in the Figure 6 and the horizontal displacement curves in the Figure 7.

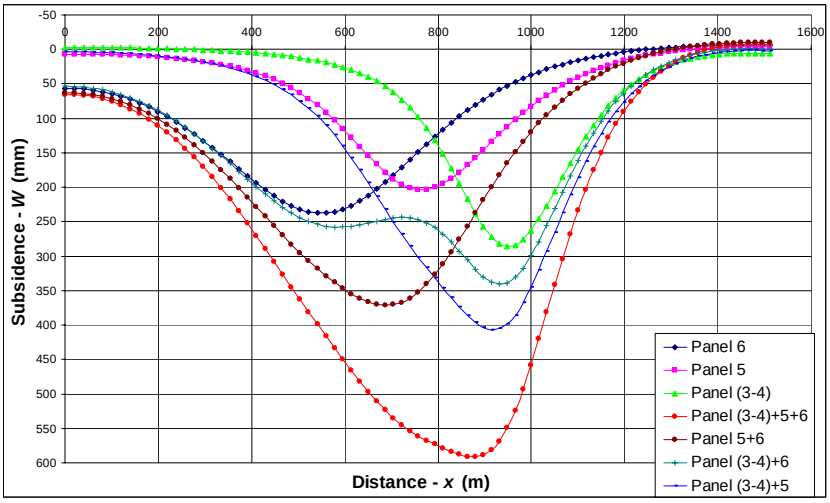

Fig. 4. Subsidence basins obtained from the numerical modelling

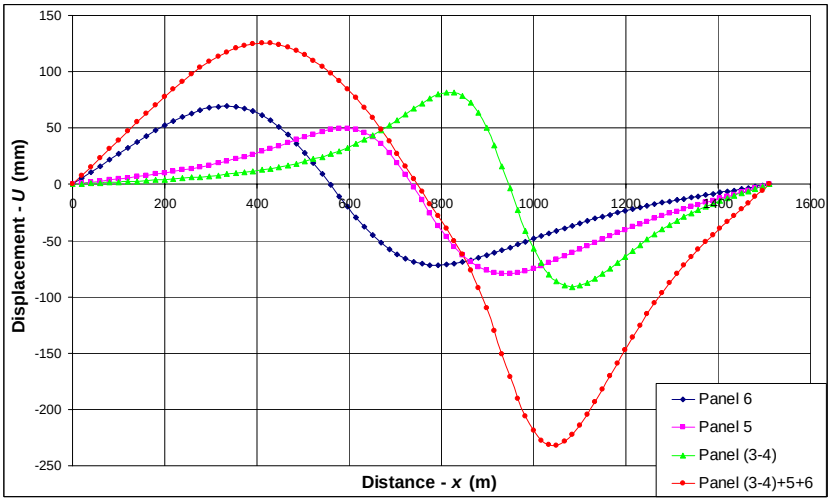

Fig. 5. Horizontal displacement graphics obtained from the numerical modelling

From the Figure 7 can be concluded the fact that between the model "with mining voids" and the model "with caved zones" there is a small difference, about of 200 mm. Also, between the same type models, computed in elasticity and elasto-plasticity, the difference is very small (negligible).

As a result of the 2D finite element modelling (CESAR-LCPC code), it is observed that the development of the subsidence basin is dynamic (Florkowska, 2010) – for example, the case of the panel (3-4), in function of the various sizes of the panel mining (figure 8 – the subsidence

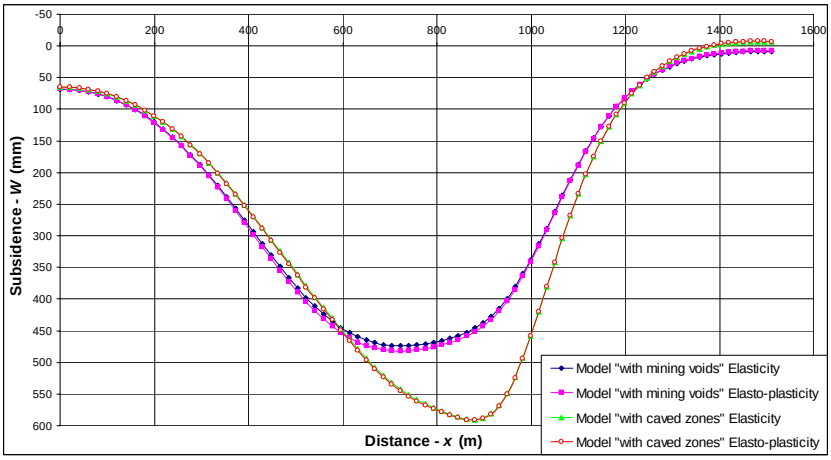

Fig. 6. Subsidence basins obtained from numerical modelling in elasticity and elasto-plasticity rocks behaviour

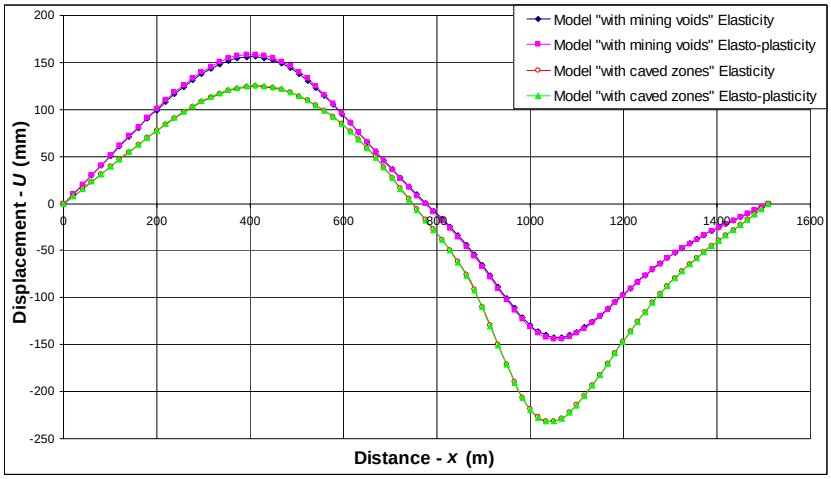

Fig. 7. Horizontal displacement graphics obtained from numerical modelling

curves; figure 9 – the horizontal displacement graphics). It is established that at the maximum size of the mined panel of about 346 m (the real panel (3-4) length) the maximum subsidence (critical subsidence) is not reached. The critical subsidence could be achieved at the 1500 m panel extension of the mining; over that size, the subsidence becomes supercritical (similarly, for the panels 5 and 6, this distance being 2000 m)**.**

In the Figures 8 and 10 was represented the maximum subsidence depending on the panel (3-4) length. The successive periods of the panel mining are the following: t = 5; 9; 13; 17; 21; 25 months (corresponding for an average face advancement speed about 14 m/month).

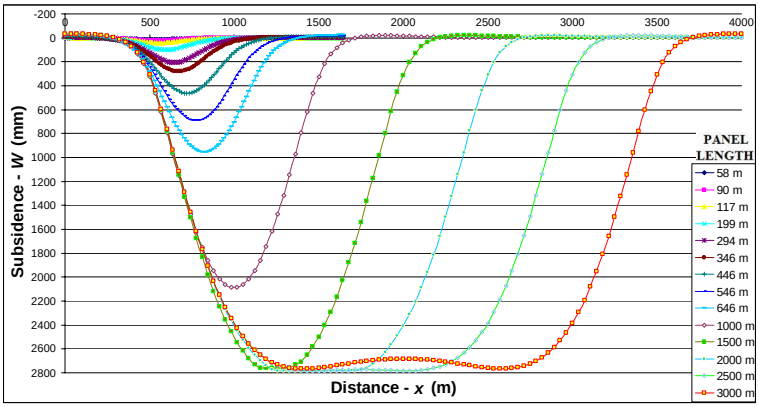

Fig. 8. Dynamic subsidence basin (coal seam no. 3, panel (3-4), Livezeni Mine)

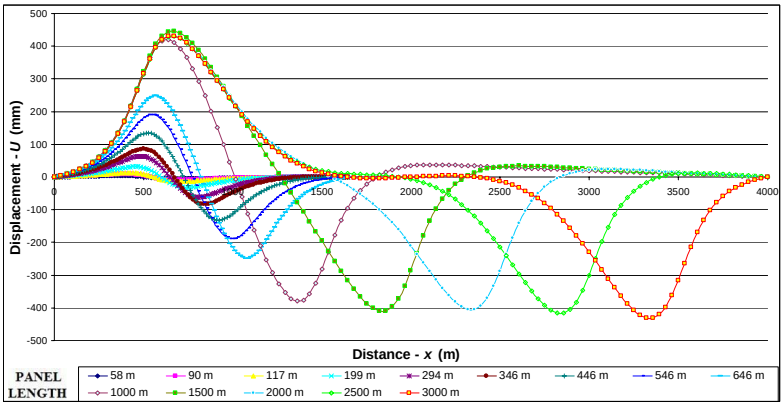

Fig. 9. Dynamic horizontal displacements (seam no. 3, panel (3-4), Livezeni Mine)

2.2.2. 3D numerical modelling of the subsidence phenomenon at the Livezeni Mine

2.2.2.1. Presentation of the 3D model

In view to achieve the spatial modelling, with the 3D finite elements, of the ground surface stability, in the case of the Livezeni Mine, the CESAR-LCPC code and the Cleo3D processor were used.

It was considered as necessary to achieve the 3D modelling of the subsidence phenomenon at the Livezeni Mine because the monitoring station of the subsidence situated at the limits of the mining goaf (Fig. 1) is less representative for the 2D modelling, in the plane strain hypothesis.

Because of the important sizes of the model it was necessary to make a simplification without very much affecting the real phenomenon development. Therefore there were made the

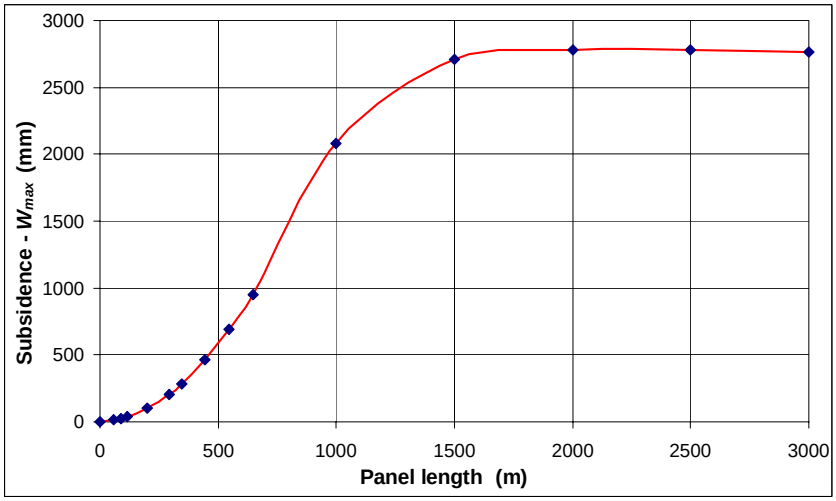

Fig. 10. Maximum subsidence in function of the panel (3-4) extension

following suppositions: it was considered the coal seam having a constant dip and thickness; the shape of the mining goaf was supposed to be a rectangular one; these three adjacent mining panels were represented as perfectly parallel; the ground surface was generated as a polygonal shape, near the real curvatures, respecting the real monitoring station levels and of the most interesting ground surface points.

From the previous 2D modelling experience resulted the inexistence of significant differences between the results obtained in the "elastic behaviour" hypothesis calculus and the "elasto-plastic behaviour" or between the two types of goaf representations (with the "mining voids" or "caved rocks"). Therefore, because of the 3D model complexity and the big computational resources, required by the elasto-plastically behaviour hypothesis of the rock massive, it was preferred to take into consideration a single model with "mining voids" in the elastic behaviour hypothesis.

2.2.2.2. Modelling achievement

The subsidence phenomenon modelling, with 3D finite elements, for the case of the Livezeni Mine, requires completion of the same stages, similarly with the 2D modelling (Onica, 2001a; Onica et.al., 2010).

For a good approximation of the results the extensive models were made with sizes of about X = 1440 m, Y = 1500 m and Z = 650 m (taking into consideration the distance of 500 m, measured from the model ends until the goaf limits, to avoid the model limits' influences on the modelling results). The model meshing, respectively of every region, was achieved by hexahedral elements with linear interpolation, resulting a total number of nodes of 95 611 and 89 244 volume elements (Fig. 11). In figure 11, there are represented only the floor rocks and the coal seam with three "mining voids", corresponding to the mining panels (3-4), 5 and 6.

For to simplify the 3D models, were taken into consideration 3 regions with different geo-mechanical characteristics, corresponding to the roof rocks, floor rocks and the coal seam.

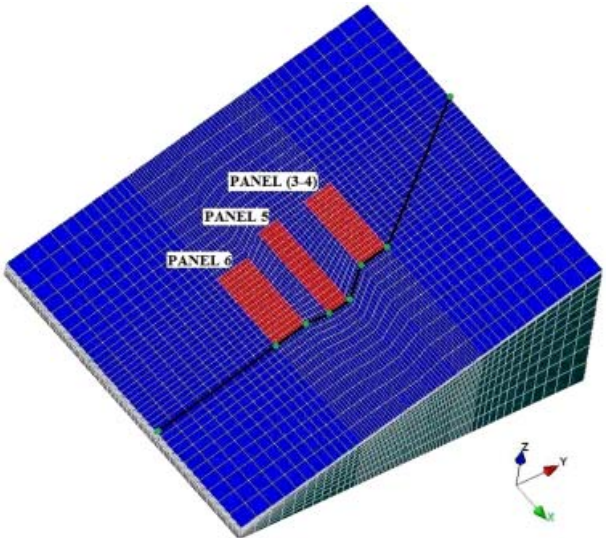

Fig. 11. 3D representation of the floor rocks, of the thick coal seam no. 3 and the "mining voids" (the black line is the monitoring station trail)

The rocks and the coal are considered to be homogenous and isotropic and are presented as average values in the Table 1 (values reduced with a structural weakness coefficient $K = 0.3$).

To impose the limit conditions the surface of the model was considered free and the inferior and lateral sides blocked (for the inferior side the vertical displacements $w = 0$ and the horizontal ones $u \neq 0$; $v \neq 0$ and for the lateral sides $w \neq 0$ and $u = 0$; $v = 0$).

In all cases of the numerical modelling, achieved in this work, the initial conditions of the model loading were considered as geostatic (Onica 2001a; Onica et. al., 2010).

2.2.2.3. Analysis of the results obtained from the numerical modelling

The subsidence basin obtained from the 3D numerical modelling is represented in Figure 12, by report to the measured subsidence, following the monitoring station (Fig. 11), and with the one computed in 2D modelling. Also, in Figure 13 is represented the horizontal displacement watching the Y axis (following the monitoring station trail – drawn with black line in Figure 11).

In Figure 12, it could be observed that the subsidence basin obtained from numerical modelling with 3D finite elements is much closer to the measured, by report to the 2D numerical modelling subsidence. The explanation is that the 2D numerical modelling subsidence is following the principal profile and the 3D subsidence is along the real measured profile (impossible to represent by 2D finite element modelling). The differences existed between the 3D modelling because of the fact that the subsidence measured at the monitoring station points is affected by a certain horizontal slip, being situated at the goaf limit.

In Figure 14 is represented the horizontal displacements after the X axis, following the monitoring station, or the transversal displacements of the points corresponding to the monitoring station.

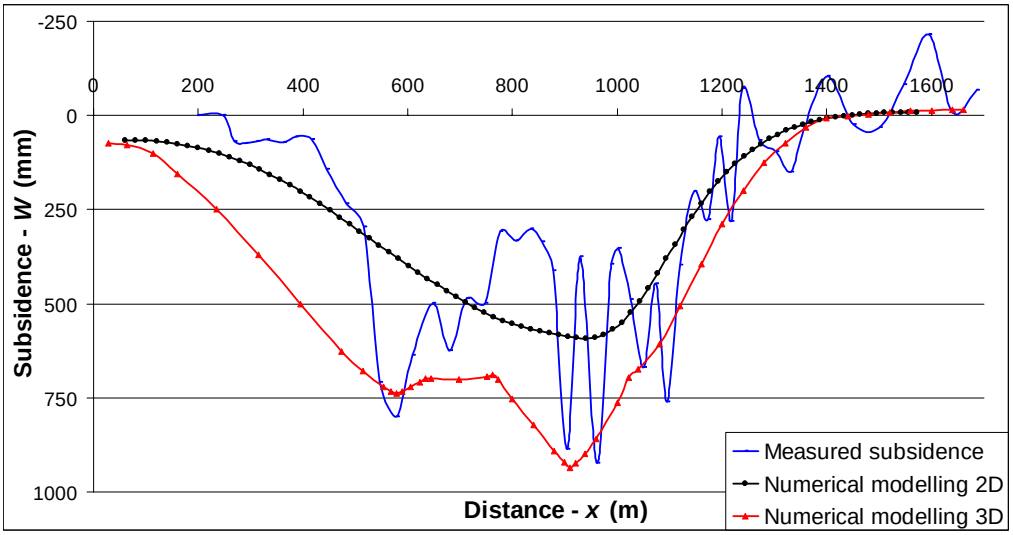

Fig. 12. Subsidence basin obtained from 2D and 3D numerical modelling, by report to the measured subsidence

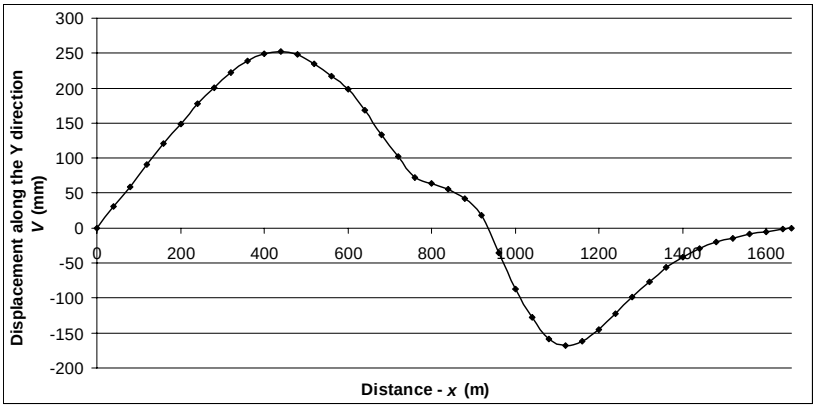

Fig. 13. Horizontal displacement curve after Y axis, obtained from 3D numerical modelling

3. Subsidence analysis in the case of the coal seam no. 3, block V, panel 1, Uricani Mine

The ground surface displacement and deformation monitoring under the underground mining influence at the Uricani Mine is achieved by the medium of the monitoring station composed of 10 observation benchmarks (the station length is of 563.6 m).

The topographical measurements were three in three months, beginning with October 2007. This monitoring station provides data concerning the ground surface displacements and

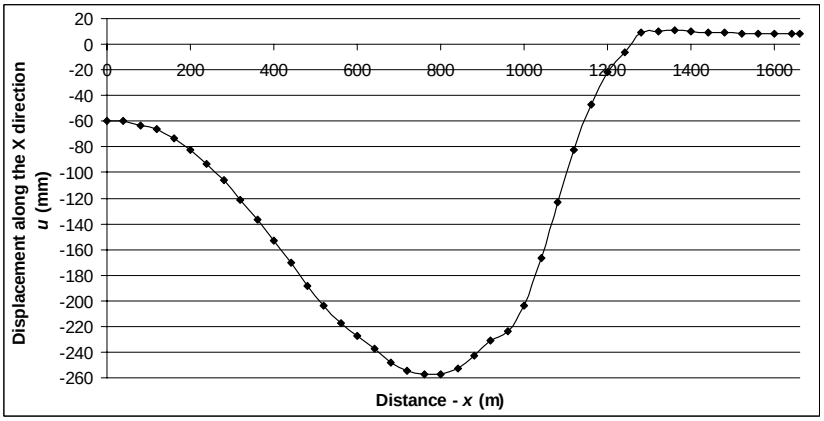

Fig. 14. Horizontal displacement curve after X axis, from 3D numerical modelling (according to the monitoring station profile)

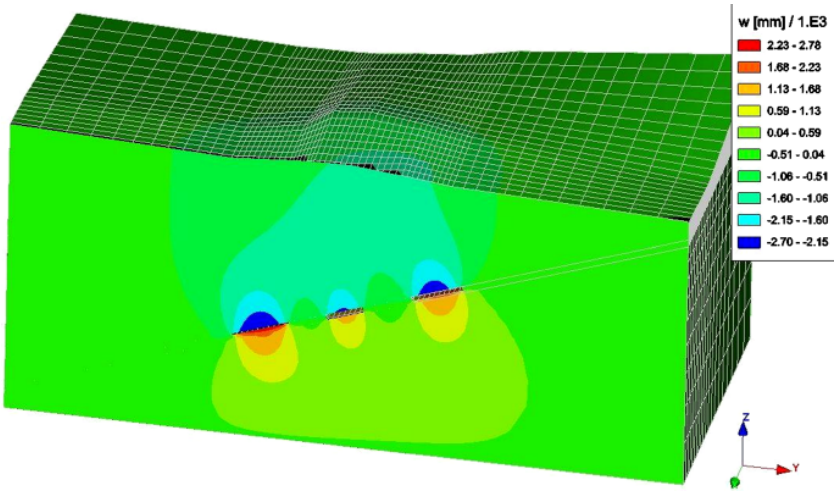

Fig. 15. Scalar representation of the subsidence, following the principal profile (in the centre of the "mining voids") *w*, in mm

deformations by consequence of the underground mining of the coal seam no. 3, block V, panel 1 (Fig. 17).

The mining of the thick and gentle inclined coal seam (of under 10^{o}) was achieved with top coal caving longwall mining (with a length of 90 m) on the entire seam thickness and on the panel length of 354 m. This panel mining began in 2003 and was completed in the second half of the year 2007.

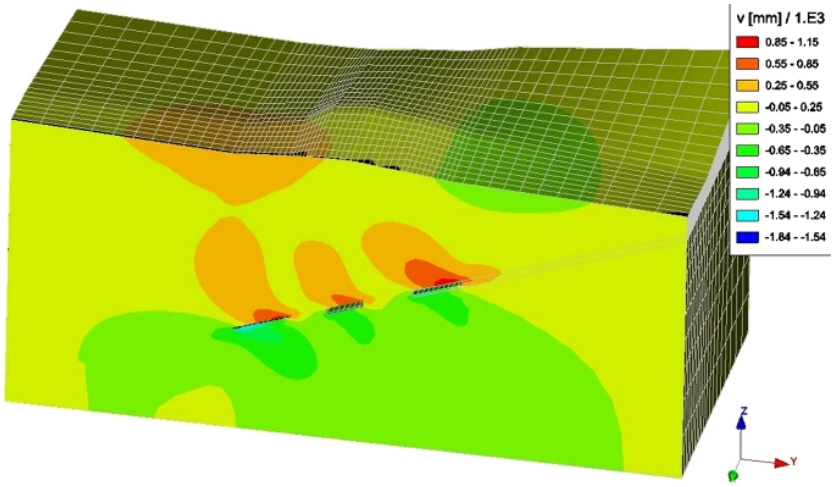

Fig. 16. Horizontal displacements in the principal profile after Y axis *v*, in mm

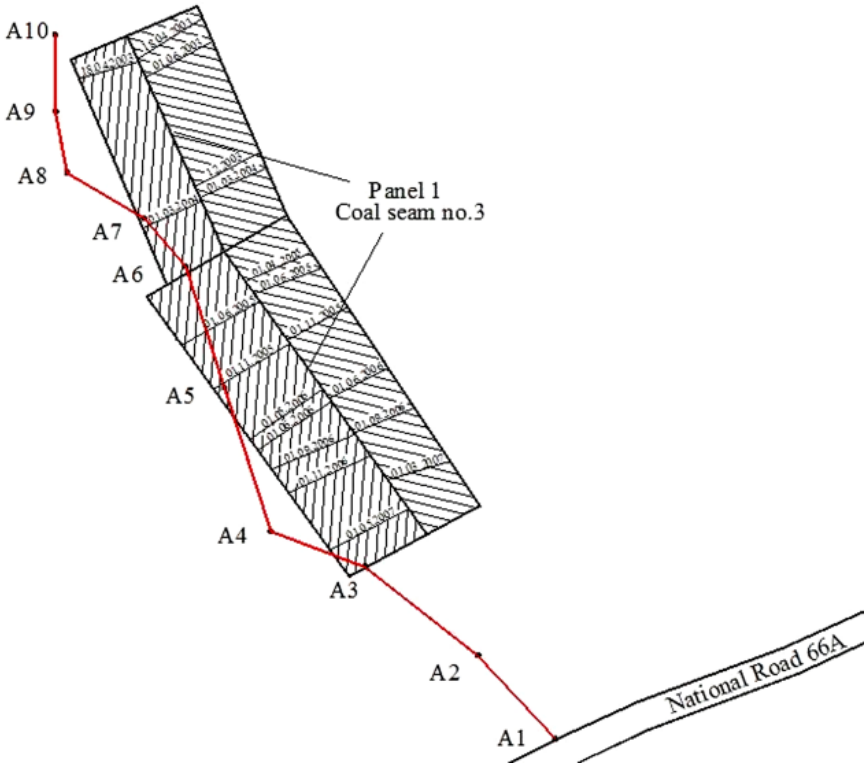

Fig. 17. Monitoring station for the ground surface subsidence at the Uricani Mine

3.1. Statistical approximation of the measurements with the aid of the profile functions

Besides the horizontal displacement U, in mm, and the horizontal strain ε, in mm/m, other important parameters which define the subsidence basin are: the subsidence or the vertical displacement, W, in mm; slope, T, in mm/m; curvature, K, in m^{-1} (Hejmanowsky & Kwinta, 2009; Kwinta, 2009; Ostrowski & Piskorz, 2009).

Studying these parameters, we found that between them there exist some dependencies, namely: the vertical displacements are maximum when the slope is zero and presents an inflexion point for a maximum value of the slope (in the point where the curvature of the subsidence basin vanishes).

For a mathematical expression of these dependencies, the following functions will be defined: $W(x)$ is the vertical displacements function; $T(x)$ – slope function; $K(x)$ – curvature function.

Thus, the measured subsidence basins were statistically analysed with the aid of a new developed profile function which has the following form:

$$W(x) = a \cdot x^b \cdot e^{-c \cdot x} \tag{1}$$

where: a, b and c are the regression coefficients.

Between these functions exists the followings mathematical correlations, namely (Onica, 2001b):

$$T(x) = \frac{dW}{dx}; \quad K(x) = \frac{d^2W}{dx^2} \tag{2}$$

Taking into account the previous correlations, depending on the regression parameters, there could be established the other parameters' equations of the subsidence basin.

$$T(x) = \frac{dW(x)}{dx} = \frac{a \cdot x^{(1-b)}}{e^{c \cdot x}} \cdot (b - c \cdot x) \tag{3}$$

For $T(x) = \frac{dW(x)}{dx} = 0$, respectively at the distance $x = \frac{b}{c}$ results the maximum subsidence:

$$W_{\max} = a \cdot \left(\frac{b}{c}\right)^b \cdot e^{-b} \tag{4}$$

Also, the curvature function of the subsidence basin is:

$$K(x) = \frac{d^2W(x)}{dx^2} = a \cdot x^{(b-2)} \cdot e^{-c \cdot x} \cdot \left[c^2 \cdot \left(x - \frac{b}{c}\right)^2 - b\right] \tag{5}$$

The inflexion points x_1 and x_2 of the vertical displacement curve (for $K(x) = 0$) are: $x_{1,2} = \frac{b \pm \sqrt{b}}{c}$

In the case of the coal seam no. 3, block V, panel 1, Uricani Mine, the coefficients a, b and c obtained for every partial subsidence profile and the square of the coefficient of determination R^2 of every equation (1) are presented in Table 4.

TABLE 4

Regression coefficients a, b and c and the coefficient of determination R^2

Data	Time – t [month]	a	b	c	R^2
03.12.2007	1.25	$4.201 \cdot 10^{-30}$	14.784333	0.041864	0.984
15.03.2008	4.6	$6.279 \cdot 10^{-23}$	11.414900	0.032404	0.986
16.06.2008	7.7	$2.494 \cdot 10^{-19}$	9.696927	0.026632	0.985
05.09.2008	10.3	$1.858 \cdot 10^{-15}$	7.950222	0.022357	0.985
15.11.2008	12.7	$1.152 \cdot 10^{-14}$	7.592713	0.021372	0.983
12.03.2009	16.5	$1.041 \cdot 10^{-14}$	7.637613	0.021582	0.968
12.06.2009	19.5	$2.522 \cdot 10^{-14}$	7.460140	0.020980	0.961
15.09.2009	22.7	$7.914 \cdot 10^{-14}$	7.247970	0.020503	0.956

To introduce the time variable into this profile function, the regression operation of the all regression coefficients, shown in the Table 3, was made, depending on the time t. Thus, there resulted a new generalized profile function, time dependent, which has the form:

$$W(x,t) = a_1 \cdot t^{a_2} \cdot x^{b_1 \cdot \ln(t) + b_2} \cdot e^{-(c_1 \cdot \ln(t) + c_2) \cdot x} \tag{6}$$

Where: x is the distance measured from the limit of the subsidence basin; t – time; $a_1 = 2 \cdot 10^{-31}$; $b_1 = -2.593$; $c_1 = -0.0074$; $a_2 = 12.936$; $b_2 = 15.365$; $c_2 = 0.0435$; ($R^2 = 0.971$) are the regression coefficients of the generalized profile function.

The real subsidence curves, depending on the time, and the results of the time dependent profile function are presented in Figure 18.

In the year 1981, Peng and Chen (Peng & Chen, 1981; Peng, 1986) developed the following negative exponential function of the subsidence profile on the major cross section of the subsidence basin:

$$W(x) = W_{\max} \cdot A \tag{7}$$

Where: $A = e^{-a \cdot z^b}$; $W_{\max}$ is the maximum subsidence; a, b are constants; $z = \frac{x}{s}$; x is the horizontal distance from the origin (which is located at the centre of the subsidence profile); s is the half-width of the subsidence basin.

Also, for the calculus of the horizontal displacement, the following relation is proposed:

$$U(x) = U_{\max} \cdot A' \tag{8}$$

Where: $A' = -a \cdot b \cdot z^{(b-1)} \cdot A$.

In our cases (when the subsidence profiles are asymmetrical), in order to obtain the complete subsidence profile, the relation (7) must be applied twice, for the left side and for the right side

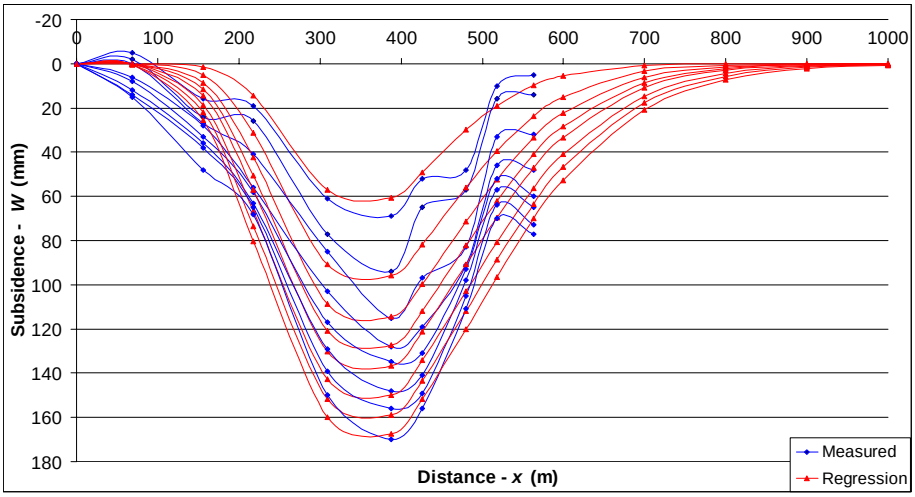

Fig. 18. Real curves of the ground subsidence and the corresponding profile functions, in the case of the coal seam no. 3, block V, panel 1, Uricani Mine

of the measured subsidence profile. If this relation is applied for every time profile, there will be obtained the corresponding regression coefficients a_s and b_s, for the left side profile, and a_d and b_d for the right side profile. Similar to the profile function (6), so as to introduce the time variable in the Peng & Chen function, the regression of the regression coefficients was made, depending on the time. Thus, the following relations were obtained:

a) for the left side of the subsidence profile:

$$W_s(x,t) = W_{\max} \cdot e^{-m_s \cdot z^{n_s}} \tag{9}$$

Where: $m_s = a_{s1} \cdot \ln(t) + a_{s2}$ and $n_s = b_{s1} \cdot \ln(t) + b_{s2}$
The obtained regression coefficients are the following: $a_{s1} = -0.936$; $a_{s2} = 6.642$; $b_{s1} = -0.074$; $b_{s2} = 2.139$ ($R^2 = 0.994$)

b) for the right side of the subsidence profile:

$$W_d(x,t) = W_{\max} \cdot e^{-m_d \cdot z^{n_d}} \tag{10}$$

Where: $m_d = a_{d1} \cdot t^{a_{d2}}$ and $n_d = b_{d1} \cdot t^{b_{d2}}$.
For the geo-mining conditions of the Uricani mine, the regression coefficients have the following values: $a_{d1} = 6.964$; $a_{d2} = -0.693$; $b_{d1} = 4.085$; $b_{d2} = -0.401$ ($R^2 = 0.983$)

The real subsidence curves, depending on the time, and the approximation results of the modified Peng & Chen time dependent profile function are presented in Figure 19.

In the previous figure, there could be observed that the Peng & Chen modified relation offers a very good fit of the measured data. The main advantage of this profile function is that it

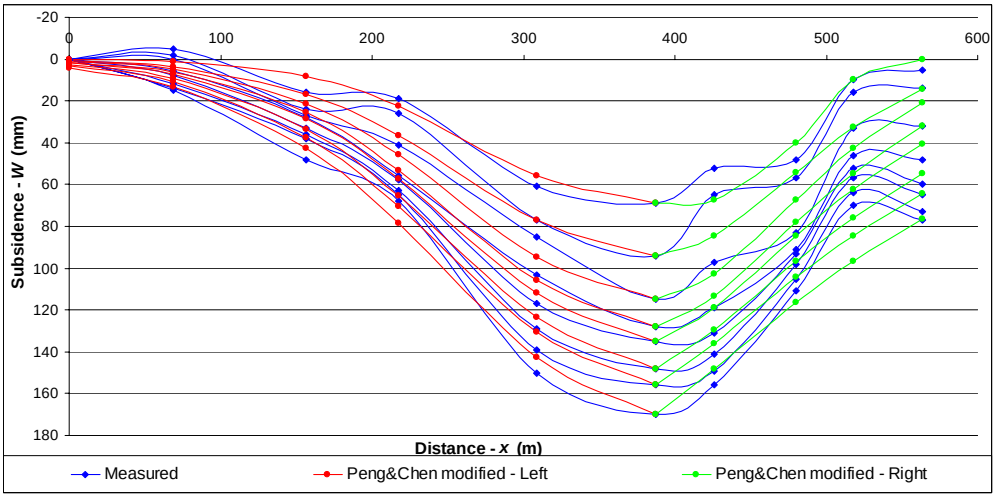

Fig. 19. Real subsidence curves and the curves of the Peng & Chen modified profile function

takes into consideration both the maximum subsidence and the time. In the case of deficiencies, it may be mentioned that: if the monitoring station didn't cover the entire profile of the subsidence basin, the function couldn't predict the behaviour of the entire subsidence profile; the connexion between every time dependent left and right profiles is through an angular point.

3.2. Numerical modelling of the subsidence phenomenon, in the case of the Uricani Mine

3.2.1. 2D finite element modelling

For to achieve the 2D finite element computational models, the CESAR-LCPC code was used, version 4 (developed by the Roads and Bridges Central Laboratory of Paris).

For to determine the ground surface subsidence and displacement, in the case of the Uricani Mine, two different models were made, in the plane strain hypothesis, namely: the first model following the seam dip (Fig. 20a), representing a vertical cross-section by the point A6, shown in the Figure 17; the second model, on the seam strike (Fig. 20b), representing a directional cross-section by the middle of the goaf space.

The calculus was made in the elasto-plastically behaviour hypothesis without hardening, assuming that both the surrounding rocks and the coal seam are continuous, homogeneous and isotropic and geo-mechanical characteristics used in the calculus are the average ones (Tab. 1). Also, the caved roof rocks were equated with a very compressible medium with $E = 15\,000$ kN/m^2 and $\nu = 0.4$.

For fitting the models depending on the measured values of the maximum vertical displacements and the adjustment of the laboratory characteristics at the in situ rocks characteristics, the calculus was made successively with reducing the characteristics values with 50%, 60% and 70% (respectively using the structural weakness coefficient $K = 0.5$; 0.4; 0.3).

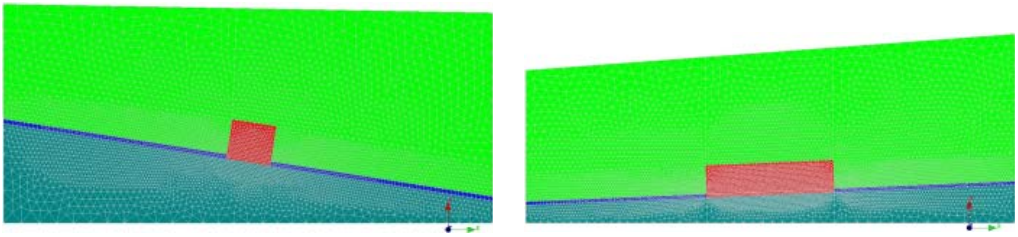

a) b)

Fig. 20. Plane strain numerical modelling of the subsidence phenomenon, in the case of the Uricani Mine: a) dip model; b) strike model

The initial loading conditions were considered as geostatic $[\sigma_o]$, corresponding to a depth of about $H = 390$ m, namely: the vertical geostatic stresses $\sigma_{oy} = 102{,}4$ MPa; the horizontal geostatic stresses $\sigma_{ox} = k_o \cdot \sigma_{oy} = 24{,}6$ MPa (where: $k_o = \frac{\nu}{1-\nu} = 0.24$). The corresponding stresses induced by the excavations are $[\sigma_e] = [-102.4; -24.6$ MPa. Finally, the models' loading was provided in the total stresses: $[\sigma_T] = [\sigma_o] - [\sigma_e]$.

In Figure 21a, there are presented the subsidence profiles obtained by the "dip model" (for the structural weakness coefficient $K = 0.5; 0.4; 0.3$), and in Figure 21b, the curves of the corresponding horizontal displacement.

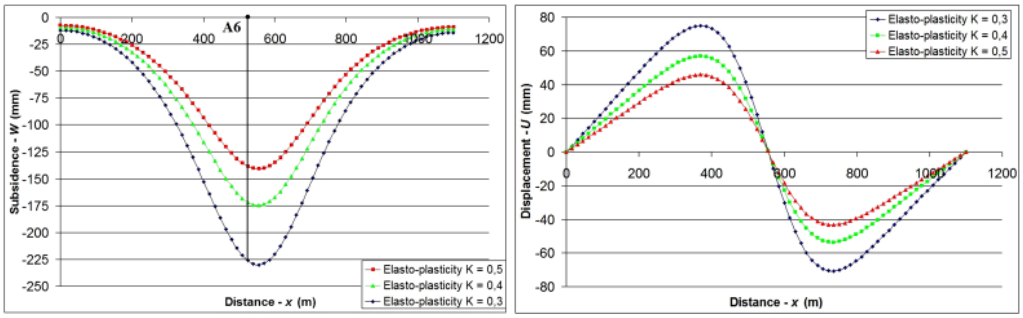

a) b)

Fig. 21. Subsidence parameters for the finite element "dip model": a) subsidence, b) displacement

From Figure 21, it could be observed that the model closest to reality is the model with the reduced characteristics with 60%. By consequence, the "strike model" was calculated, in the Mohr-Coulomb elasto-plastic behaviour hypothesis, taking into account a structural weakness coefficient $K = 0.4$.

In the "strike model", for to represent the third dimension (the panel width) $\lambda = 0.4$ was introduced, a coefficient for reducing the stresses of mining void $[\sigma_e]$ with about 60%.

The subsidence basin of the numerical model was compared with measured subsidence (Fig. 22), resulting an equal maximum subsidence but with certain deviation from the general subsidence profile.

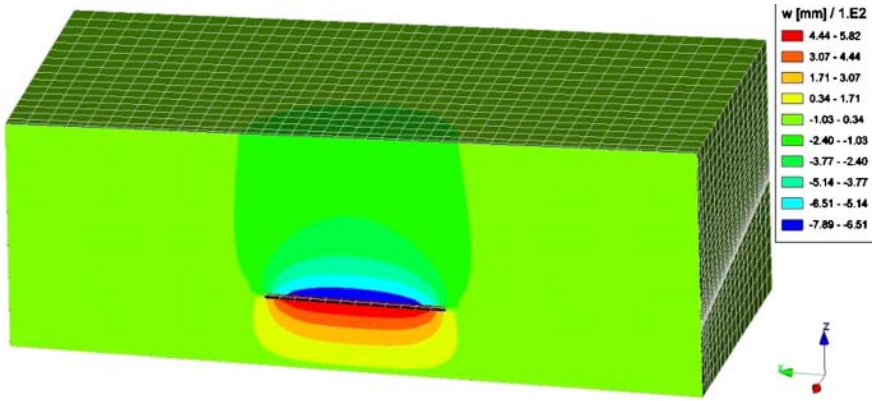

Fig. 22. Subsidence basin obtained from the numerical modelling compared with the real measured subsidence profiles

3.2.2. 3D finite element modelling of the subsidence phenomenon at the Uricani Mine

As in the previous case, from the Livezeni Mine, for to achieve the 3D analysis of the ground surface stability, affected by the underground mining of thick coal seam no. 3, panel 1, block V, at the Uricani Mine, the same computational code was used. Thus, a single model was created, with "mining voids", in the hypothesis of the elastic behaviour of the rock massive.

The achievement of the 3D modelling goes through the same steps as required in the previous case.

For a better precision of the calculus the models were made with the sizes of X = 1354 m, Y = 1100 m and Z = 470 m, taking a distance of 500 m from the nodel ends to the edge of goaf. The model meshing, respectively of every region, was realized by hexahedral finite elements with linear interpolation (with 48 711 nodes and 44 800 volume elements).

Also, there were taken into consideration 3 regions with different averages (pondered with every rocks' thickness), corresponding to the roof and floor rocks and the coal seam, for to simplify the 3D model geo-mechanical characteristics.

On the basis of the same arguments, as in the previous modelling cases, the initial loading conditions of the model were geostatic [σ_o] (corresponding to an average depth of H = 390 m), namely: vertical geostatic stresses σ_{oz} = 102,4 MPa; horizontal geostatic stresses $\sigma_{oz} = \sigma_{oy}$ = 24.6 MPa.

The subsidence basin obtained by the numerical modelling, with 3D finite elements, following the ground surface monitoring station trail (Fig. 23) is shown in figure 22, in comparison with the measured subsidence and the results from the 2D numerical modelling (in the principal profile).

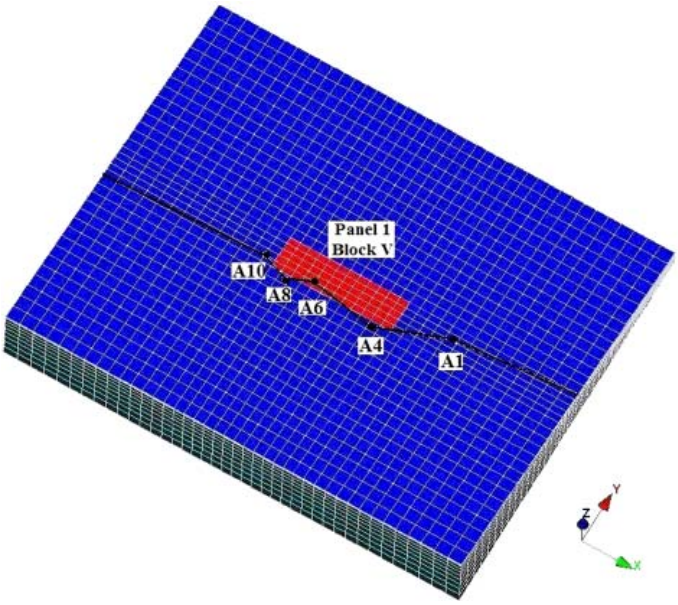

Fig. 23. Monitoring station trail in report to the "mining void" location

Also, in figure 24a is represented the variation of the horizontal displacements after X axis and in figure 24b, after Y axis (transversal on the monitoring station).

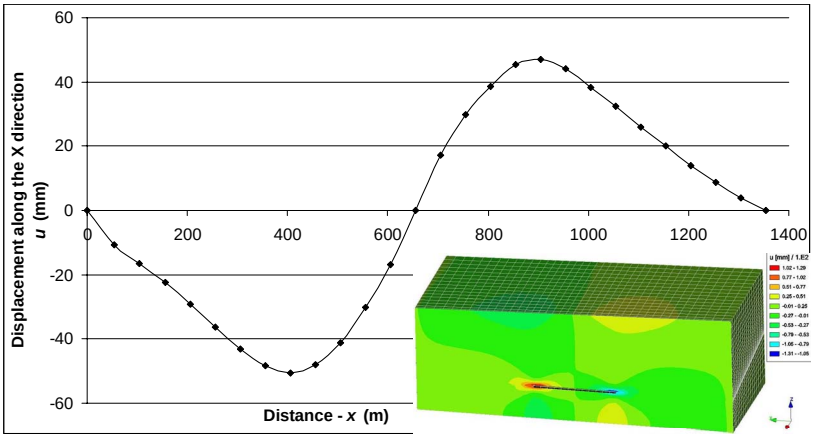

Fig. 24a. Horizontal displacements after X axis, obtained from 3D numerical modelling

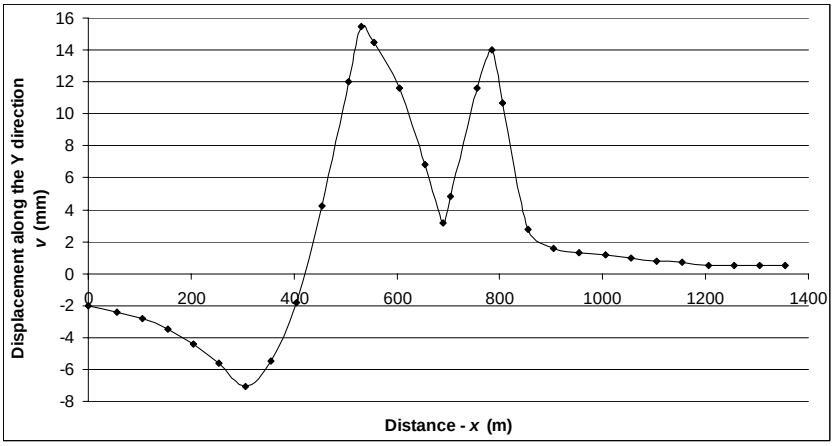

Fig. 24b. Horizontal displacements after Y axis, obtained from 3D numerical modelling (transversal on the monitoring station)

4. Subsidence analysis in the case of the coal seam no. 3, block VII-VIII, face no. 366 and 376, Vulcan Mine

The monitoring of the ground surface subsidence under the influence of underground mining at the Vulcan Mine is made by aid of the monitoring station composed of 16 benchmarks (the total length of the monitoring station being of 620.8 m). The topographical observations were executed in a number of three in three months, beginning with October 2008. This monitoring station provides the data concerning the ground surface subsidence and deformation data as a consequence of the underground mining of coal seam no. 3, block VII-VIII, faces no. 366 and 376 (Fig. 25).

Coal seam no. 3 (with an average thickness of about 50 m) is mined in horizontal slices with top coal caving mining method, related with these two coal faces. The mining began in 1964, when the roof control by rocks caving was used.

After the statistical analysis of the measurements and the approximation of these with the aid of the profile function (1), then after the regression operation of the regression coefficients of every measurement stage, the generalized profile function (6) was obtained, time dependent, with the following regression coefficients:

$a_1 = 7 \cdot 10^{-132}$; $b_1 = -4.1863$; $c_1 = -0.0113$; $a_2 = 21.23$; $b_2 = 60.35$; $c_2 = 0.1363$ ($R^2 = 0.950$).

The subsidence curves, periodically measured, as well as the approximation curves of the time dependent profile function is graphically represented in Figure 26, where it is shown a very good fit of the in situ measurements.

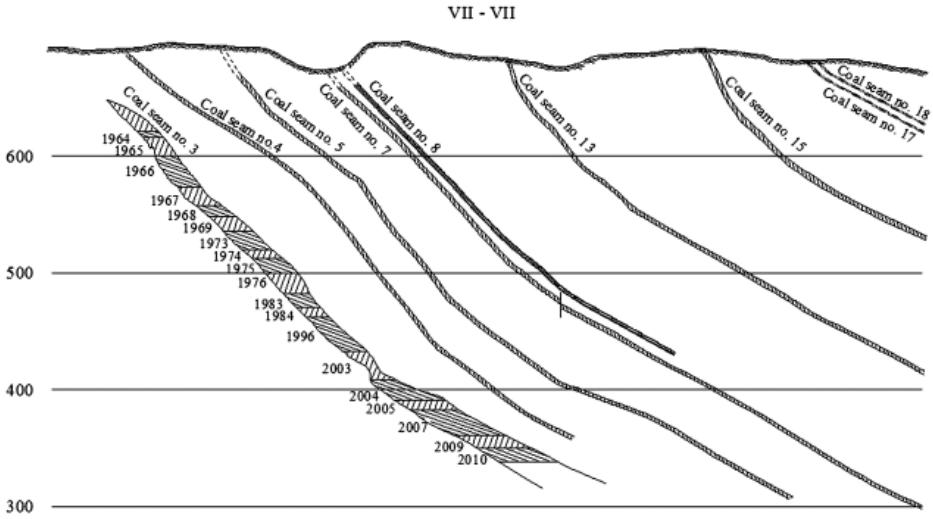

Fig. 25. Vertical cross – section, Vulcan Mine

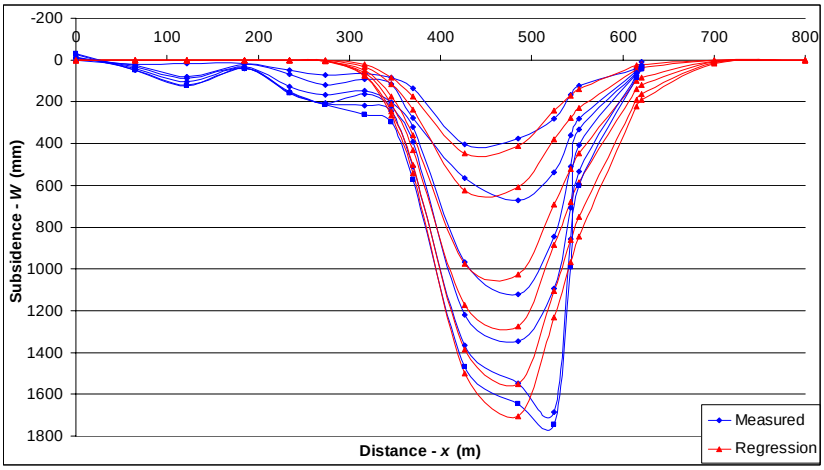

Fig. 26. Real subsidence curves and the curves of the time dependent profile function, in the case of coal seam no. 3, block VII-VIII, face no. 336 and 376, Vulcan Mine

5. Subsidence analysis in the case of the coal seam no. 3 and 5, block VI, Lonea Mine

Hereinafter, the measurement achieved on an old monitoring station will be analysed, materialized in the year 1985 by the Mining Faculty of Petroşani. This station is composed of two alignments: one strike alignment with a single stable end composed of 14 benchmarks (with a

total length about 380 m) and one transversal alignment with a single stable end, composed of 35 benchmarks (with a total length about 558 m). The strike alignment was monitored until the year 1987, when the stable benchmark was lost and on the strike alignment the observation was made until the year 1996.

This monitoring station provides the data concerning the ground subsidence as effect of the mining of coal seam no. 3 and 5, block VI (Fig. 27). The average dip of the coal seams is of about 30° and the thickness is 28-42 m, for the coal seam no. 3 and 4-5 m, for coal seam no. 5. The applied mining method is in horizontal slices, with roof control by integral rocks caving.

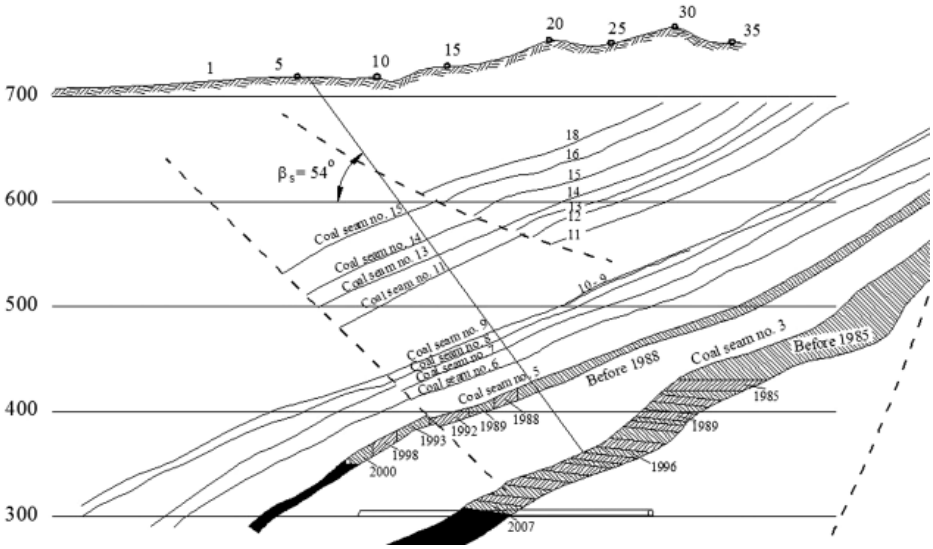

Fig. 27. Transversal cross-section trough the coal deposit of the Lonea Mine

Similarly with the previous cases, the regression coefficients of the generalized time dependent profile function (6) are the following:

$$a_1 = 3 \cdot 10^{-123};\ b_1 = -8.527;\ c_1 = -0.013716;\ a_2 = 46.949;\ b_2 = 54.017;$$
$$c_2 = 0.095607\ (R^2 = 0.970).$$

Also in this case, it is observed a good statistical approximation of the real measurements with this profile function.

The subsidence curves, in time measured, as well as the statistical approximation with the generalized profile function (6) are graphically represented in Figure 28.

As it is shown in Figure 28, because of the advancement in the deep of the mining of coal deposit, the position of the point, corresponding to the maximum subsidence, for every intermediary subsidence profile, is modified and the subsidence basin develops asymmetrically, and more laterally.

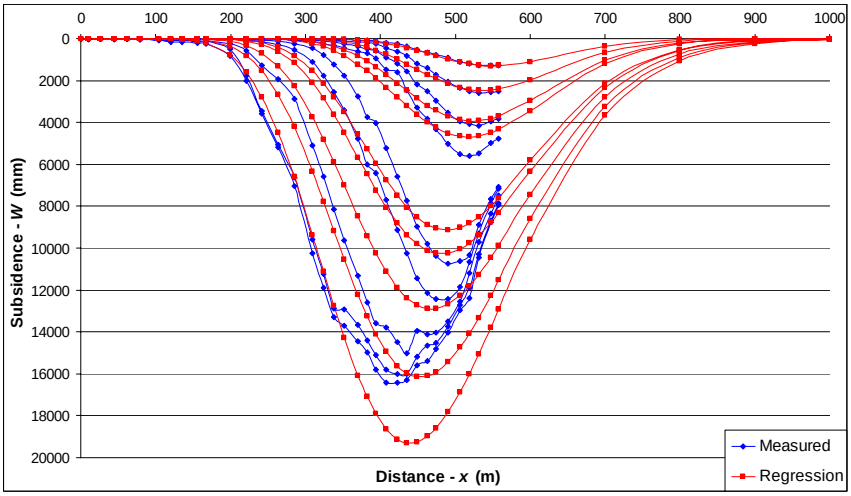

Fig. 28. Subsidence curves, time dependent, measured and approximated with the profile function, for the case of coal seam no.3 and 5, block VI, Lonea Mine

6. Subsidence analysis in the case of the coal seam no. 3, face no. 138 and 139, Petrila Mine

The measurements made along the alignment 200, materialized in year 1981, are composed of 16 monitoring benchmarks, disposed on the distance of 250 m. Since 1978, the coal seam no. 3 mining, under the level +300 m, was practiced by slices, using the roof control by caving at the area of face no. 138 and 139. During the year 1991, in the face no. 139 was achieved the total filling at the level +200 m (Ortelecan, 1997).

Similar with the previous cases, the statistical analysis of the measurements was made by profile function (1) and the generalized time dependent function (6) which led to the following regression coefficients:

$$a_1 = 2.676 \cdot 10^{-4};\ b_1 = -0.364;\ c_1 = -0.002496;\ a_2 = 2.414;\ b_2 = 2.828;$$
$$c_2 = 0.019876\ (R^2 = 0.981).$$

The subsidence curves of the real data and the results of the profile function, defined by the previous coefficients, are represented in Figure 29.

7. Subsidence analysis in the case of the coal seam no. 3, block III, Dâlja Mine

In this case it will be analysed the measurement achieved on a monitoring station that was materialized in the year 1975, composed of a transversal alignment with two stable ends, involving 33 benchmarks, along a distance of 841.8 m.

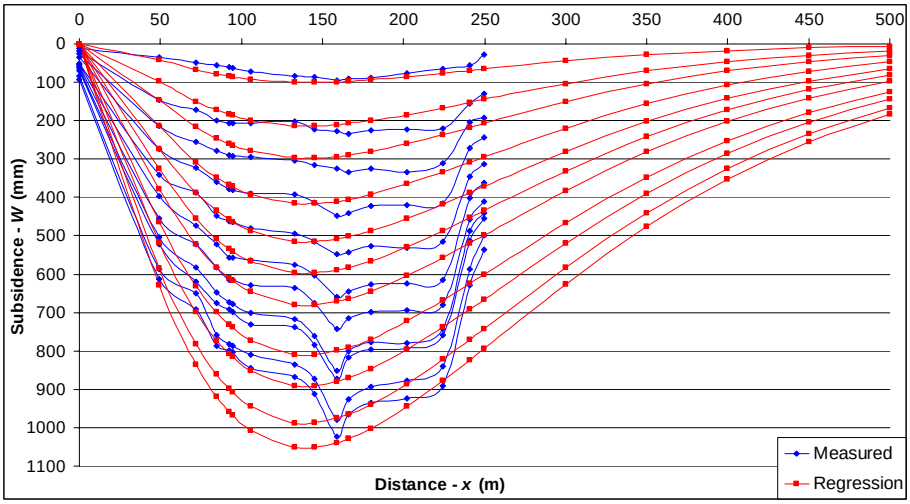

Fig. 29. Subsidence curves of the measured and approximated values, for the case of coal seam no. 3, face no. 138 and 139, Petrila Mine

The observations, on this monitoring station, were made biannually, until 1981. This station had the role of observing the ground subsidence and displacements caused by the underground mining of coal seam no. 3, block III, mined in horizontal slices and roof control by rocks caving. In this block the coal seam no. 3 has the thickness ranging between 2 and 11 m and the dip of about 60-68° (Ortelecan, 1997).

As in the cases previous presented, the statistical analysis led to the profile function (6), explicit in function of the time, with the aid of the following regression coefficients:

$$a_1 = 3.860 \cdot 10^{-140};\ b_1 = -11.879;\ c_1 = -0.024739;\ a_2 = 62.418;\ b_2 = 63.180;$$
$$c_2 = 0.135407\ (R^2 = 0.865).$$

The subsidence curves, measured and approximated, are shown in Figure 30.

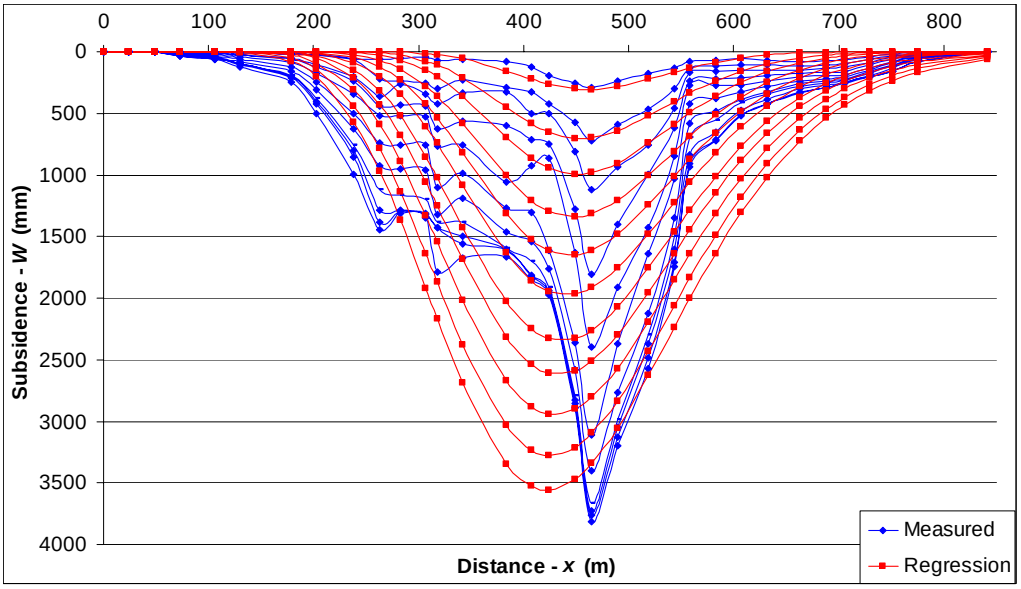

Fig. 30. Subsidence curves, depending on the time, in the case of coal seam no. 3, block III, Dâlja Mine

8. Conclusions

At the same time with the reconsideration of the mining of Jiu Valley hard coal deposit, because of the closing programme of several mines and the beginning of a new panels' mining and the need for the revalorization of the surface lands and the assessment of the constructions' integrity, the requirement of assessment of the ground surface stability has arisen, in the mining fields influence areas.

Therefore, an immediate assessment of the measurements provided over time was tried, in the different Jiu Valley mining fields and the analysis of this data base, stored by the Hard Coal Company of Petroşani (some significant case studies are presented in this paper).

We mention that the data analysis was difficult because the ground surface monitoring was made following the alignments that were not always relevant from a scientific point of view. Over time, the purpose of this monitoring was to observe the stability of certain roads, land areas and other targets of immediate interest.

By consequence, a time dependent profile function was elaborated, which predicts very well the development in time of the subsidence basins produced as an effect of the underground mining of the thick coal seams of the Jiu Valley coal basin. Also, with the encouraging results, we tried to adapt, at the Jiu Valley conditions, the profile function made by Peng and Chen for the Northern Appalachian Coalfield.

Along with the profile function method, in some case studies, we called upon the numerical modelling with the aid of the 2D plain strain and 3D finite element method. The calculus was made in elasticity and elasto-plasticity with the models "with mining voids" and "with caved zones".

After the sensibility analysis and the fitting of the models, significant results were obtained for the geo-mining conditions of the Jiu Valley coal basin.

The subsidence phenomenon analysis by the profile functions methods, by numerical modelling and other researches tools will be further developed, at the entire coal basin level. These are the prediction and control methods, necessary for the new panels mining design and the measures required to mitigate the degradation phenomenon of the lands situated under the influence areas of the underground mining fields.

References

Almăşan B., 1984. *The Mining of Romanian Mineral Resources Deposits, Tom I* (in Romanian), Technical Publishing House, Bucharest, pp. 70-291.

Covaci St., 1983. *Underground Mining, Tom I* (in Romanian), Didactical and Pedagogical Publishing House, Bucharest, 424 p.

Florokowska L., 2010. *Land Subsidence Due to Mining Operations in Disturbed Rock Mass, on the Example of Ruda Slaska (Poland)*, Arch. Min. Sci., Vol. 55, No. 3, pp. 691-701.

Hejmanowsky R., Kwinta A., 2009. *Determining the Coefficient of Horizontal Displacements with the Use of Orthogonal Polynomials*, Arch. Min. Sci., Vol. 54, No. 3, pp. 441-454.

Hirean C., 1981. *Rocks Mechanics* (in Romanian), Didactical and Pedagogical Publishing House, Bucharest, 322 p.

Kwinta A., 2009. *Transitivity Postulate Effect on Function of Influences Range Radius in Knothe Theory*, Arch. Min. Sci., Vol. 54, No. 1, pp. 135-143.

Oncioiu G., Onica I., 1999. *Ground Deformation in the Case of Underground Mining of Thick and Dip Coal Seams in Jiu Valley Basin (Romania)*, Proceedings of 18th International Conference on Ground Control in Mining, 3-5 August, 1999, Morgantown, WV, USA, pp. 330-336.

Onica I., 2001a. *Introduction in the Numerical Methods Used in the Mining Excavations Stability Analysis* (in Romanian), Universitas Publishing House, Petroşani, 156 p.

Onica I., 2001b. *Environmental Mining Impact* (in Romanian), Universitas Publishing House, Petroşani, pp. 173-198.

Onica I., Cozma E., Goldan T., 2006. *Land Degradation Under the Underground Mining Influence* (in Romanian), AGIR Revue, year XI, no. 3, pp. 14-27.

Onica I., Cozma E., 2008. *Stress and Strain State Developed Around the Longwall Faces in the Jiu Valley Coal Basin*, Proceedings of the 21 World Mining Congress & Expo – Session 6: Coal Mining – Chances and Challenges, Krakow, pp. 153-163.

Ortelecan M., 1997. *The Study of Ground Surface Displacement Under the Underground Mining of Jiu Valley Coal Deposits – Eastern Zone* (in Romanian), Ph.D. Thesis, University of Petroşani, 195 p.

Ortelecan M., Pop N., 2005. *Topographical Methods for Buildings and the Ground Surfaces Behaviour Surveying* (in Romanian) AcademicPres Publishing House, Cluj-Napoca, 256 p.

Ostrowski J., Piskorz M., 2009. *Characterization of the Asymmetry of Knothe Model Distributions of Deformations Indexes*, Arch. Min. Sci., Vol. 54, No. 4, pp. 753-774.

Todorescu A., 1984. *Rocks Properties* (in Romanian), Technical Publishing House, Bucharest,676 p.

Peng S.S., 1986. *Coal Mine Ground Control*, John Wiley and Sons, New York, pp. 420-460.

Peng S.S., Chen D.W., 1981. *Analysis of Surface Subsidence Parameters Due to Underground Longwall Mining in the Northern Appalachian Coalfield*, Department of Mining Engineering, West Virginia University, TR 81-12, 22 p.

Petrescu I. e.a., 1987. *The Coal Deposits Geology, Tom 2* (in Romanian), Technical Publishing House, Bucharest, pp. 81-106.

Received: 28 June 2011